

Distinctive Higgs Signals of a Type II 2HDM at the LHC

Shinya Kanemura^{1 *}, Stefano Moretti^{2 †}, Yuki Mukai^{1 ‡}, Rui Santos^{2 §} and Kei Yagyu^{1 ¶}

¹ *Department of Physics, University of Toyama, 3190 Gofuku, Toyama 930-8555, Japan.*

² *School of Physics and Astronomy, University of Southampton, Highfield, Southampton SO17 1BJ, UK.*

(Dated: November 18, 2018)

We perform a numerical analysis of Higgs-to-Higgs decays within a Type II 2-Higgs Doublet Model (2HDM), highlighting several channels that cannot occur in its Supersymmetric version, thereby allowing one to possibly distinguish between these two scenarios. Our results are compliant with all available experimental bounds from both direct and indirect Higgs searches and with theoretical constraints from vacuum stability and perturbative unitarity.

I. INTRODUCTION

Whilst Supersymmetry (SUSY) [1] provides an attractive theoretical scenario for physics beyond the Standard Model (SM) (in its ability to remedy the hierarchy problem, to provide a natural dark matter candidate, to enable high scale gauge coupling unification, etc.), there is to date no evidence for it. In its minimal (in terms of particle content and gauge structure) incarnation, the Minimal Supersymmetric Standard Model (MSSM) [2], SUSY is highly predictive though, e.g., in the Higgs sector. Of the initial eight degrees of freedom pertaining to the two complex Higgs doublets responsible for Electro-Weak Symmetry Breaking (EWSB) in the MSSM, after the latter has taken place, three are consumed to give mass to the $SU(2) \otimes U(1)$ weak gauge bosons, W^\pm and Z , so that five physical Higgs states survive: the CP-neutral ones h and H ($M_H > M_h$), the CP-odd one A and the charged states H^\pm . In effect, regarding the Higgs sector, the MSSM is nothing but a 2-Higgs Doublet Model (2HDM) of Type II (in the nomenclature of Ref. [3]), whereby SUSY enforces relations amongst Higgs masses and couplings, on the one hand, and weak gauge boson masses and interaction parameters, on the other hand, in such a way that, of the original 7 independent parameters defining a CP-conserving 2HDM (see below), only two survive as such in the MSSM [4]. These can be taken to be $\tan\beta$, the ratio of the Vacuum Expectation Values (VEVs) of the two Higgs doublet fields, and one of the extra Higgs boson masses. At tree-level, these are the only inputs needed to compute Higgs masses and couplings to ordinary matter (quarks, leptons and gauge bosons) as well as Higgs self-couplings. Hence, if SUSY had chosen all the sparticle masses to be much larger than the SM objects and the Higgs bosons, so that they are not accessible at the upcoming Large Hadron Collider (LHC), one intriguing question to ask would be whether it is possible to distinguish between the MSSM and a Type II 2HDM on the sole basis of Higgs interactions with SM matter and/or self-interactions. Or, conversely, whether it would be possible to dismiss the assumption of such (decoupled) heavy sparticles, hence of minimal SUSY altogether (aka the MSSM), from the observation of particular signals in the Higgs sector alone.

It is the purpose of this work to prove that this is the case, exploiting the fact that SUSY prevents some Higgs-to-Higgs decays, that remain instead possible in a generic Type II 2HDM. This is primarily connected to the fact that a generic pattern of Higgs masses, as dictated by SUSY, in the MSSM is the one in which the h is rather light (in fact, below 130 GeV or so, for heavy sparticles [5]) whilst the others (H , A and H^\pm) are quite heavy and degenerate in mass, the more so the larger $\tan\beta$ [33]. In fact, even in the presence of off-shellness effects [6, 7] in all decay products in Higgs decay chains in the MSSM, essentially only the $H \rightarrow hh$ and $A \rightarrow Zh$ channels are possible in this scenario [34]. In contrast, in a

* kanemu@sci.u-toyama.ac.jp

† stefano@phys.soton.ac.uk

‡ mukai@jodo.sci.u-toyama.ac.jp

§ rsantos@cii.fc.ul.pt

¶ keiyagyu@jodo.sci.u-toyama.ac.jp

Type II 2HDM without SUSY, many other decays are possible, e.g.:

$$\begin{aligned} H &\rightarrow AA, & H &\rightarrow H^+ H^-, & H &\rightarrow W^\pm H^\mp, & H &\rightarrow ZA, \\ & & A &\rightarrow W^\pm H^\mp, & A &\rightarrow ZH, \\ H^\pm &\rightarrow W^\pm h, & H^\pm &\rightarrow W^\pm H & H^\pm &\rightarrow W^\pm A. \end{aligned} \quad (1)$$

While the existence of such different decay patterns in the two models has been known for some time [4], our ultimate intention here is to prove that the 2HDM Type II is still phenomenologically viable in the light of all available experimental constraints. In practise then, whilst, of course, these decays could not all occur at the same time, depending on the Type II 2HDM parameters, a subset of them would be possible, therefore providing a means of distinguishing between the two scenarios discussed, further considering that – under the above assumption of a heavy SUSY spectrum – the dominant production channels of both neutral and charged Higgs bosons in both scenarios are the same and proceed via interactions with SM particles [8, 9].

The plan of the paper is as follows. In the next section we describe the Type II 2HDM that we will be using and we fix our conventions. The following section discusses the experimental and theoretical bounds. We then illustrate our results quantitatively in section IV. The final section outlines the conclusions.

II. THE TWO-HIGGS DOUBLET MODEL

We start with a brief review of the 2HDM used in this work. The potential chosen is the most general, renormalisable and invariant under $SU(2) \otimes U(1)$ that one can build with two complex Higgs doublets with a softly broken Z_2 symmetry. It can be written as

$$\begin{aligned} V_{\text{2HDM}} = & \mu_1^2 |\Phi_1|^2 + \mu_2^2 |\Phi_2|^2 - (\mu_3^2 \Phi_1^\dagger \Phi_2 + \text{h.c.}) \\ & + \frac{1}{2} \lambda_1 |\Phi_1|^4 + \frac{1}{2} \lambda_2 |\Phi_2|^4 + \lambda_3 |\Phi_1|^2 |\Phi_2|^2 + \lambda_4 |\Phi_1^\dagger \Phi_2|^2 + \frac{\lambda_5}{2} \left\{ (\Phi_1^\dagger \Phi_2)^2 + \text{h.c.} \right\}, \end{aligned} \quad (2)$$

where Φ_1 and Φ_2 are the two Higgs doublets with hypercharge $+1/2$ and μ_3^2 is the Z_2 soft breaking term. For simplicity we can take μ_3^2 and λ_5 to be real. The doublet fields are parameterised as

$$\Phi_i = \begin{bmatrix} \omega_i^+ \\ \frac{1}{\sqrt{2}}(v_i + h_i + iz_i) \end{bmatrix} \quad (i = 1, 2), \quad (3)$$

where the VEVs v_1 and v_2 satisfy $v_1^2 + v_2^2 = v^2 \simeq (246 \text{ GeV})^2$. Assuming CP-conservation, this potential has 8 independent parameters. However, because v is fixed by the W^\pm boson mass, only 7 independent parameters remain to be chosen, which we take to be M_h , M_H , M_A , M_{H^\pm} , $\tan \beta$, α (the mixing angle between the two CP-even neutral Higgs states) and $M^2 = \mu_3^2 / (\sin \beta \cos \beta)$ (which is a measure of how the discrete symmetry is broken). The definition of α and β and the relation among physical scalar masses and coupling constants are shown in Ref. [10] for definiteness.

In a general 2HDM, the Yukawa Lagrangian can be built in four different and independent ways so that it is free from Flavour Changing Neutral Currents (FCNCs). We define as Type II the model where ϕ_2 couples to up-type quarks and ϕ_1 couples to down-type quarks and leptons [35]. (We present the Yukawa couplings for a Type II 2HDM in the Appendix.)

III. EXPERIMENTAL AND THEORETICAL BOUNDS

The results from all LEP collaborations on topological searches with two Higgs bosons or one Higgs and one gauge boson were presented in Ref. [12]. We will use the experimental limits on the cross sections for $e^+ e^- \rightarrow H_1 Z$ and $e^+ e^- \rightarrow H_1 H_2$, where H_1 can be any CP-even Higgs boson and H_2 can be either a CP-even or a CP-odd Higgs boson. As we are concerned here with a Type II 2HDM, there is a bound particularly relevant to our analysis which is the one obtained from the relation involving the following cross sections (σ) and Branching Ratios (BRs):

$$\frac{\sigma(e^+ e^- \rightarrow H_1^{2\text{HDM}} Z)}{\sigma(e^+ e^- \rightarrow H_1^{\text{SM}} Z)} \text{BR}(H_1^{2\text{HDM}} \rightarrow b\bar{b}) = \sin^2(\alpha - \beta) \text{BR}(H_1^{2\text{HDM}} \rightarrow b\bar{b}). \quad (4)$$

In a Type II 2HDM $h \rightarrow b\bar{b}$ is the dominant decay for most of the parameter space for M_h below the SM limit. The two subleading competing decays are $h \rightarrow c\bar{c}$ and $h \rightarrow \tau^+\tau^-$. In a Type II 2HDM, the ratio $\Gamma(h \rightarrow b\bar{b})/\Gamma(h \rightarrow \tau^+\tau^-)$ is the SM one. In contrast, one has

$$\frac{\Gamma(h \rightarrow b\bar{b})}{\Gamma(h \rightarrow c\bar{c})} = \frac{m_b^2}{m_c^2} \tan^2 \alpha \tan^2 \beta \quad (5)$$

in the limit $m_h \gg m_q$. If we then take the case $\alpha \approx \beta$ and because we always consider $\tan \beta > 1$ the decay $h \rightarrow b\bar{b}$ becomes even more dominant in a Type II 2HDM, with respect to the SM case. Conversely, if $\alpha \approx \beta + \pi/2$, then we recover the SM ratio. Either way, $h \rightarrow b\bar{b}$ is the dominant decay by an amount which is at least the corresponding SM ratio of BRs with respect to the other fermionic decays. Because its dependence on the other parameters of the model is very mild, this essentially provides a limit in the $\beta - \alpha$ versus M_h plane. In particular, it is straightforward to check that when $\sin(\beta - \alpha) \approx 0.1$ there is essentially no bound on the lightest Higgs boson mass, while for $\sin(\beta - \alpha) \approx 0.2$ the limit immediately jumps to $M_h > 75.6$ GeV.

In this study the masses of the charged Higgs boson and the CP-odd one will always be above 200 GeV and therefore not constrained at all by the LEP bounds from direct searches. In some cases though, the mass of the heavy CP-even Higgs boson will be allowed to be below 200 GeV. In those instances we have confirmed that the LEP bounds do not apply to the cases presented in this work. Concerning H^\pm states, apart from a model independent LEP bound of $M_{H^\pm} \gtrsim M_{W^\pm}$, D0 and CDF have model dependent limits on the charged Higgs mass (see Ref. [13]) from top decays, but again these are below the range of H^\pm masses discussed in this work. No other experimental bounds exist from direct searches for the set of parameters that we will present.

Other than limits from direct searches for Higgs bosons, there are indirect constraints from precision observables, from both LEP and SLC. New contributions to the ρ parameter stemming from Higgs states [14] have to comply with the current limits from precision measurements [15]: $|\delta\rho| \lesssim 10^{-3}$. There are limiting cases though, related to an underlying custodial symmetry, where the extra contributions to $\delta\rho$ vanish. In this study we will consider two such particular cases: (A) the one where $M_{H^\pm} = M_A$ and (B) the one where $M_{H^\pm} = M_H$ with $\sin(\beta - \alpha) = 1$. These parameter choices correspond to the case in which the custodial symmetry ($SU(2)_L \otimes SU(2)_R \rightarrow SU(2)_V$) is preserved in the Higgs potential, so that the latter can be written in terms of $\text{Tr}(M_i M_i^\dagger)$ with $M_i = (i\tau_2 \Phi_i^*, \Phi_i)$ where the M_i 's ($i = 1, 2$) are translated as $M_i \rightarrow M'_i = g_L^\dagger M_i g_R$ with $g_{L,R} \in SU(2)_{L,R}$ (A) or $\text{Tr}(M_{21} M_{21}^\dagger)$ and $\det(M_{21})$, with $M_{21} = (i\tau_2 \Phi_2^*, \Phi_1)$, where M_{21} is translated as $M_{21} \rightarrow M'_{21} = g_L^\dagger M_{21} g_R$ with $g_{L,R} \in SU(2)_{L,R}$ (B), respectively [16]. In Fig. 1, we show the allowed region under the ρ parameter constraint in several scenarios which are relevant to our later discussions. Furthermore, it has recently been shown in Ref. [17] that, for a Type II 2HDM, data on $B \rightarrow X_s \gamma$ imposes a lower limit of $M_{H^\pm} \gtrsim 250$ GeV, which is essentially $\tan \beta$ independent. Other experimental constraints on a Type II 2HDM come from the results on $(g - 2)_\mu$ (the muon anomalous magnetic moment) [18], R_b (the b -jet fraction in $e^+e^- \rightarrow Z \rightarrow \text{jets}$) [19, 20], the decay $B^+ \rightarrow \tau^+\nu$ [21], $B_q \bar{B}_q$ mixing [17] and the τ leptonic decay [22]. In general, bounds from these observables can be important for relatively small values of M_{H^\pm} and large $\tan \beta \gtrsim 10$ [18, 19, 20, 21, 22, 23, 24]. Values of $\tan \beta$ smaller than ≈ 1 are disallowed both by the constraints coming from $Z \rightarrow b\bar{b}$ and from $B_q \bar{B}_q$ mixing.

Concerning theoretical constraints we will take all masses M_h , M_H , M_A and M_{H^\pm} to be below 700 GeV. This is a consequence of tree-level unitarity bounds [25, 26] in the limit $M = 0$. Furthermore, the most general set of conditions for the Higgs potential to be bounded from below are [27]

$$\lambda_1 > 0, \quad \lambda_2 > 0, \quad \sqrt{\lambda_1 \lambda_2} + \lambda_3 + \min(0, \lambda_4 - |\lambda_5|) > 0. \quad (6)$$

Recently, it was in fact proven that these are necessary and sufficient conditions to assure vacuum stability of the potential at tree level [28]. Vacuum stability against charge breaking is also built into a Type II 2HDM model, as a non-charge breaking minimum, when it exists, is always the global one in any 2HDM [29]. Finally, according to [30], perturbativity for the top and bottom Yukawa couplings forces $\tan \beta$ to lie in the range $0.3 \leq \tan \beta \leq 100$, though it turns out that, from enforcing perturbativity also on the λ_i 's, moderate values of $\tan \beta$ ($\tan \beta \sim \mathcal{O}(1)$) are preferred, especially for $M \sim 0$ GeV.

In the following, we will consider M_{H^\pm} to be 250 GeV or larger and take $\tan \beta \sim 1$ –3, so that all the Type II 2HDM scenarios presented are free from these bounds. We will show that even with such small values of $\tan \beta$ a lot of the parameter space is already excluded. This does not mean that larger values of $\tan \beta$ are not allowed but rather that they are less likely to occur. Choosing a large $\tan \beta$ forces a

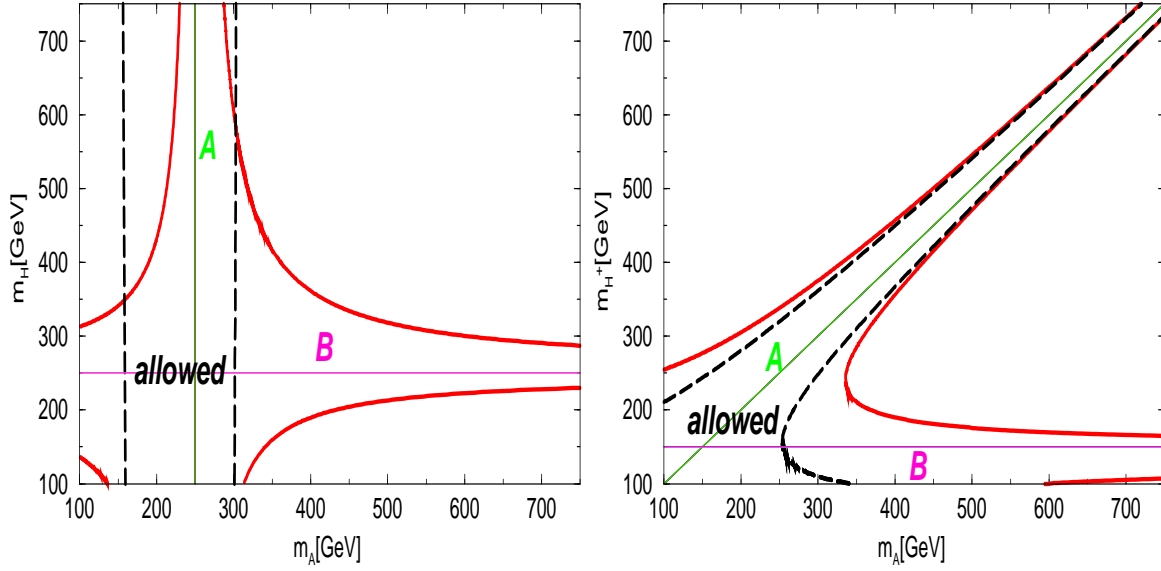


FIG. 1: Allowed regions under the ρ parameter data (at 2σ level). [Left figure] The area surrounded by solid curves corresponds to the allowed regions for the case of $M_h = 120$ GeV, $M_{H^\pm} = 250$ GeV, $\sin(\beta - \alpha) = 1$. The one surrounded by dashed curves corresponds to the allowed regions for the case of $M_h = 50$ GeV, $M_{H^\pm} = 250$ GeV, $\sin(\beta - \alpha) = 0.1$. [Right figure] The area surrounded by solid curves corresponds to the allowed regions for the case of $M_h = 120$ GeV, $M_H = 150$ GeV, $\sin(\beta - \alpha) = 0.9$. The one surrounded by dashed curves corresponds to the allowed regions for the case of $M_h = 50$ GeV, $M_H = 150$ GeV, $\sin(\beta - \alpha) = 0.1$.

very particular set of values for the remaining free parameters if one is to comply with all constraints. Therefore it may seem we are just scanning over small corners of the 2HDM parameter space. This is not the case. The 2HDM is already tightly constrained by experiment and it becomes severely constrained when one adds the theoretical bounds, especially those from perturbative unitarity. The EW precision data are also very restrictive. As shown in Fig. 1 (left), where we have fixed the mass of the charged Higgs at 250 GeV, a vast range of values of the heavy CP-even Higgs is possible. The allowed region for the pseudo-scalar masses depends on the values of $\beta - \alpha$: when $\sin(\beta - \alpha) \approx 1$ (full curve) all values of M_A are allowed provided M_H is close to $M_{H^\pm} = 250$ GeV. As we move away from $\sin(\beta - \alpha) = 1$ (dashed curve) the range of allowed values of the pseudo-scalar mass shrinks to a region around the value of $M_{H^\pm} = 250$ GeV as wide as the precision measurements permit. On the right plot we see exactly the same trend but now in the M_{H^\pm} vs M_A plane. In the plots shown in the following sections we choose the exact limits that cancel the ρ parameter contribution. We note however that we have explicitly checked that varying the values of the masses complying with these constraints does not produce a qualitative change in our analysis. In most cases not even a quantitative change is noticed. We end this section by underlining once more that we are not focusing on a small corner of the 2HDM parameter space. Considering all constraints a 2HDM Type II is subject to and the above discussion it is clear that we are spanning the entire parameter range allowed. When we focus on a definite limit, like $M_{H^\pm} = M_A$, it is for illustrative purposes only.

IV. DECAYS

Let us start by saying that all the widths and BRs presented in this work are calculated at tree-level except for the decays to $g\gamma$ (plus $\gamma\gamma$ and $Z\gamma$, not visible though in our plots) which are one-loop processes at the lowest order. However, we take into account the leading one-loop QCD corrections to Higgs to quark-antiquark decays by computing one-loop running masses for the (anti)quarks in the Yukawa couplings, evaluated at the decaying Higgs mass.

A. A decays

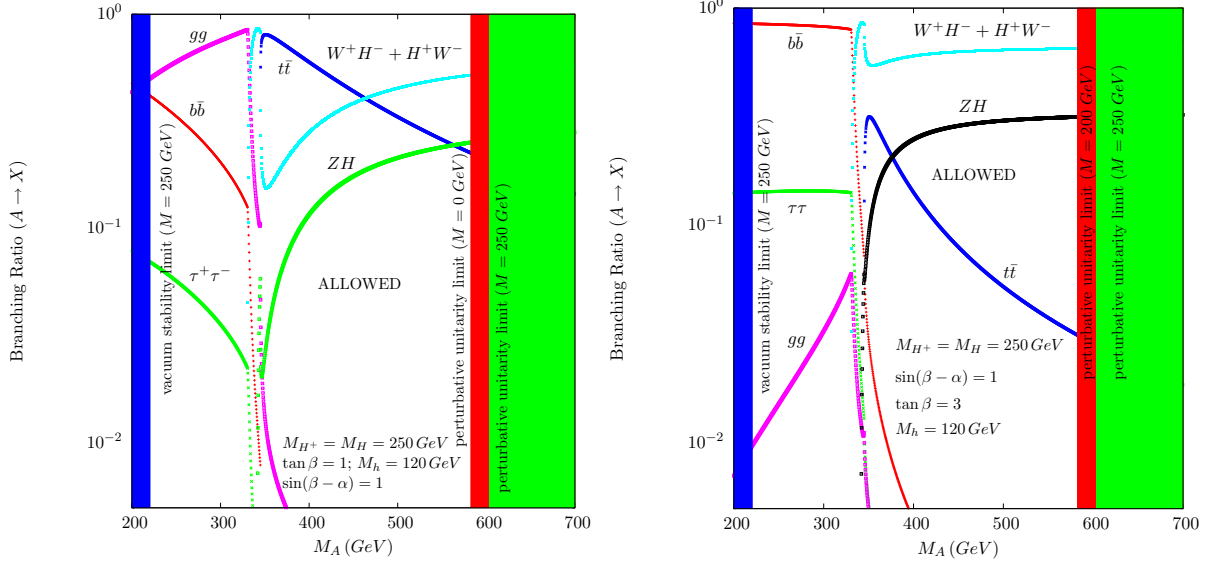


FIG. 2: A decays for $M_h = 120$ GeV, $M_H = M_{H^\pm} = 250$ GeV and $\sin(\beta - \alpha) = 1$. On the left is the plot for $\tan \beta = 1$ while on the right we set $\tan \beta = 3$. We show the perturbative unitarity limits for $M = 0$ GeV and $M = 250$ GeV on the left plot and for $M = 200$ GeV and $M = 250$ GeV on the right plot. For $M = 0$ GeV and $\tan \beta = 3$ all parameter space is excluded. We also show the vacuum stability limits for $M = 250$ GeV. For $M = 200$ GeV and below all parameter space is allowed in what concerns vacuum stability.

For the CP-odd scalar and in the mass region chosen, $\sin(\beta - \alpha)$ has to be very close to 1, in order for the model to be consistent with experimental data. Even a value of $\sin(\beta - \alpha) = 0.9$ is enough to violate precision measurements via the ρ parameter. Therefore the decay $A \rightarrow Zh$ is not allowed. We take $M_h = 120$ GeV but the CP-odd Higgs boson profile does not depend on the light CP-even Higgs boson mass. We have chosen $M_H = M_{H^\pm} = 250$ GeV due to the $B \rightarrow X_s \gamma$ bound and to the ρ constraint. Fig. 2 illustrates the decay patterns of the CP-odd Higgs state for two values of $\tan \beta$. Two comments are in order here. Firstly, notice that to choose larger values for M_H and M_{H^\pm} would only have the effect that the corresponding channels would open later. Secondly, the dependence on $\tan \beta$ is generally as follows: the larger $\tan \beta$ the more suppressed the decay into $t\bar{t}$ and consequently the CP-odd Higgs state decays more and more into other Higgs bosons as soon as the corresponding channels are kinematically allowed. All decay channels shown in these plots do not depend on M , as no Higgs self-couplings are involved in those processes. However, both the perturbative unitarity and the vacuum stability bounds depend on the value chosen for M . The excluded regions due to the the above constraints for the three values of $M = 0, 200$ and 250 GeV are shown in Fig. 2. Note that the smaller the parameter M is the smaller $\tan \beta$ has to be to avoid the perturbative unitarity limit. On the contrary, the smaller M is, the less constrained is the parameter space from the vacuum stability conditions (for $M = 0$ GeV no bounds apply).

In the MSSM, for $\tan \beta = 3$, the pseudo-scalar decays mainly to fermion pairs, $b\bar{b}$ in the low mass region and $t\bar{t}$ when the channel becomes kinematically allowed in most of the studied scenarios [31]. There is a situation where the MSSM and the general 2HDM are hard to distinguish. The branching ratio of $A \rightarrow ZH$ can be very similar in both models when we compare the so-called intermediate-coupling regime of the MSSM ($\tan \beta \approx 3$ and H/A masses below the $t\bar{t}$ threshold) with a 2HDM with a large charged Higgs mass so that the decay to W^+H^- is forbidden. In Fig. 3 we show the total A width for the two situations presented in Fig. 2. When the A decays mainly to $b\bar{b}$ or $g\bar{g}$ the width is negligible but, when the $t\bar{t}$, the other Higgs or Higgs plus gauge boson channels open, Γ_A grows rapidly reaching 100 GeV for $M_A = 700$ GeV. Note that the theoretical constraints shown in Fig. 2 are not shown again in this plot.

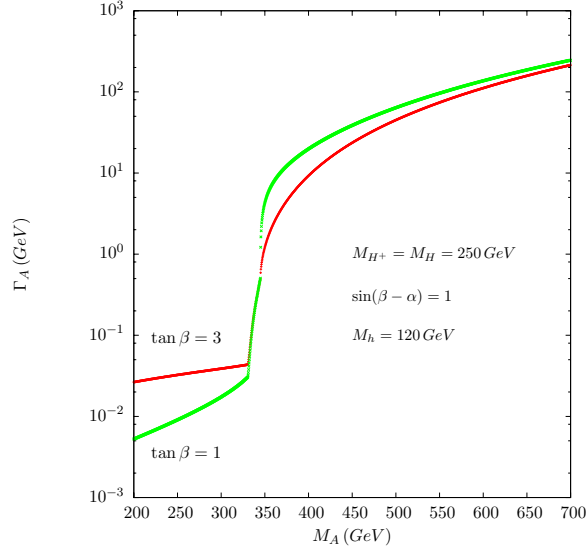


FIG. 3: Total width of the CP-odd Higgs state A for the parameter values presented in Fig. 2.

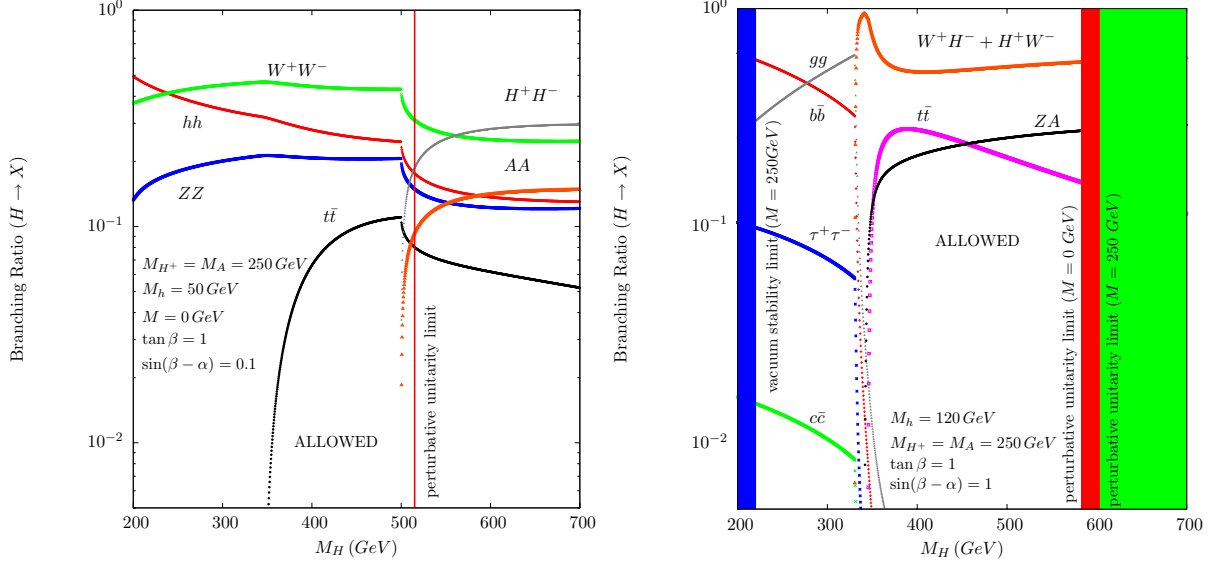


FIG. 4: H decays for $M_A = M_{H^\pm} = 250$ GeV and $\tan\beta = 1$. On the left is the plot for $M_h = 50$ GeV and $\sin(\beta - \alpha) = 0.1$ while on the right we have $M_h = 120$ GeV and $\sin(\beta - \alpha) = 1$. We show the perturbative unitarity and the vacuum stability limits, for $M = 0$ GeV for the left plot and for $M = 0$ GeV and $M = 250$ GeV for the right plot.

B. H decays

In this section we deal with the decays of the heavier CP-even Higgs boson. New contributions to the ρ parameter are avoided by setting $M_A = M_{H^\pm} = 250$ GeV. We note once more that, as shown in Fig. 1, this limit can be relaxed. As a consequence the dominant channel can be either the one with a charged Higgs or the one with a pseudo-scalar boson depending on the relation between the respective masses. Again, the constraint from $B \rightarrow X_s \gamma$ is used. Then, we distinguish between two extreme situations. The first one, shown in Fig. 4 (left), is for $\sin(\beta - \alpha) = 0.1$. In this case, the H couplings to the gauge bosons are close to the SM ones. Due to the small value of $\sin(\beta - \alpha)$ the mass bound on the light Higgs can easily be evaded and we choose the mass $M_h = 50$ GeV (though smaller masses are also allowed). This is also the limit where the H couplings to $W^\pm H^\mp$ and ZA are very small. In this left plot we can distinguish

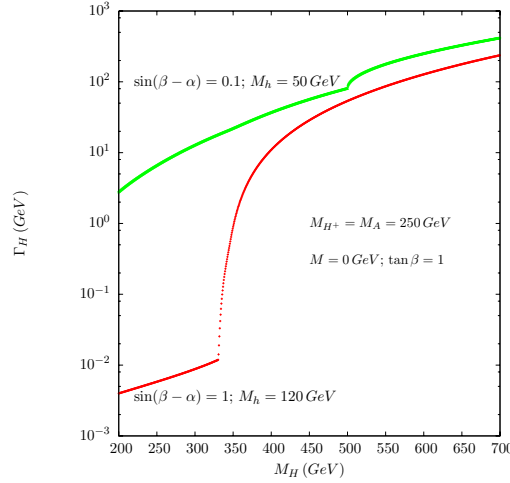


FIG. 5: Total width of the CP-even heavy Higgs state H for the parameter values presented in Fig. 4.

two interesting regions with new physics signatures. For small H masses, $H \rightarrow hh, W^+W^-, ZZ$ can be the dominant decays. For large H masses, the decays to a pair of charged Higgs bosons and to a pair of CP-odd Higgs states dominate as soon as they are kinematically allowed (though for a small M_H interval). The larger $\tan\beta$ is the more dominant these decays become. We also present the perturbative unitarity limit for $M = 0 \text{ GeV}$. We still present the decays that are above the perturbative unitarity limit for two reasons. Firstly, because as M grows the allowed M_H region also grows (although for, for example, for $M = 200 \text{ GeV}$, the $H \rightarrow hh$ channel is negligible and in the low H mass region $H \rightarrow W^+W^-$ always dominate) and the decay to two charged Higgs and/or two pseudo-scalars are then allowed over a much larger M_H interval. Secondly, because, had we chosen a lower value for M_A and M_{H^\pm} , the corresponding decays would have opened for lower M_H values, hence well within the region allowed by perturbative unitarity.

The other extreme situation is shown on the right hand side of Fig. 4 and occurs for $\sin(\beta - \alpha) = 1$. In this limit, the H couplings to the gauge bosons are exactly zero. Decays to the two light Higgs states are also suppressed but they could still play a role if the soft breaking parameter is different from zero. This is the limit where H couplings to $W^\pm H^\mp$ and ZA are largest. Again we show perturbative unitarity and vacuum stability constraints for this case. Notice that the choice of $\tan\beta = 1$ is heavily imposed by these bounds: for $\tan\beta = 2$ and for the same set of parameters shown in the plot, the heavy CP-even Higgs mass is forced to be below $\approx 350 \text{ GeV}$. Even if M is raised to 200 GeV the bound only grows to $\approx 400 \text{ GeV}$. In Fig. 5 we show the total H width for the two situations presented in Fig. 4. When $M_h = 50 \text{ GeV}$, left plot in Fig. 4, the heavy Higgs is allowed to decay to other Higgs and gauge bosons and that is why the H width is SM-like for the same mass. In the other scenario the heavy CP-even Higgs is not allowed to decay to gauge bosons. It decays to two gluons and fermion pairs in the low mass region. Therefore the H width is much smaller. As soon as channels with Higgs and gauge boson open both widths converge to similar values.

In the MSSM, for $\tan\beta > 1$, the heavy Higgs decays mainly to fermion pairs $b\bar{b}$ and then $t\bar{t}$ in the decoupling regime. Outside this regime there are two particular cases where distinguishing between both models will be hard. The first one is the anti-decoupling regime ($\tan\beta \gtrsim 10$ and $M_A \lesssim M_h^{max}$) where, if kinematically allowed, the $H \rightarrow hh$ can be the dominant decay channel. Hence, a 2HDM Higgs as presented in the left plot of Fig. 4 can be mistaken by such a MSSM heavy Higgs. The same is true for the above described intermediate-coupling regime where $Br(H \rightarrow hh)$ reaches 60 % for a significant heavy Higgs mass region. For a detailed discussion see [31].

C. H^\pm decays

This section is dedicated to charged Higgs boson decays. Again, we choose $M_{H^\pm} = M_A$ to avoid the constraints from the ρ parameter. Once more we distinguish between two extreme cases regarding the

value of $\sin(\beta - \alpha)$, which is the parameter that regulates the H^\pm coupling to other Higgses and gauge bosons. When $\sin(\beta - \alpha)$ is such that the LEP bounds can be avoided there are mainly two competing decays for the allowed charged Higgs boson mass region: $H^+ \rightarrow t\bar{b}$ and $H^+ \rightarrow W^+h$. In Fig. 6 we show the charged Higgs BRs for $\sin(\beta - \alpha) = 0.1$ and $M_h = 50 \text{ GeV}$ for two values of $\tan\beta$. It is clear that the decay $H^+ \rightarrow W^+h$ is always important and becomes dominant for large values of $\tan\beta$.

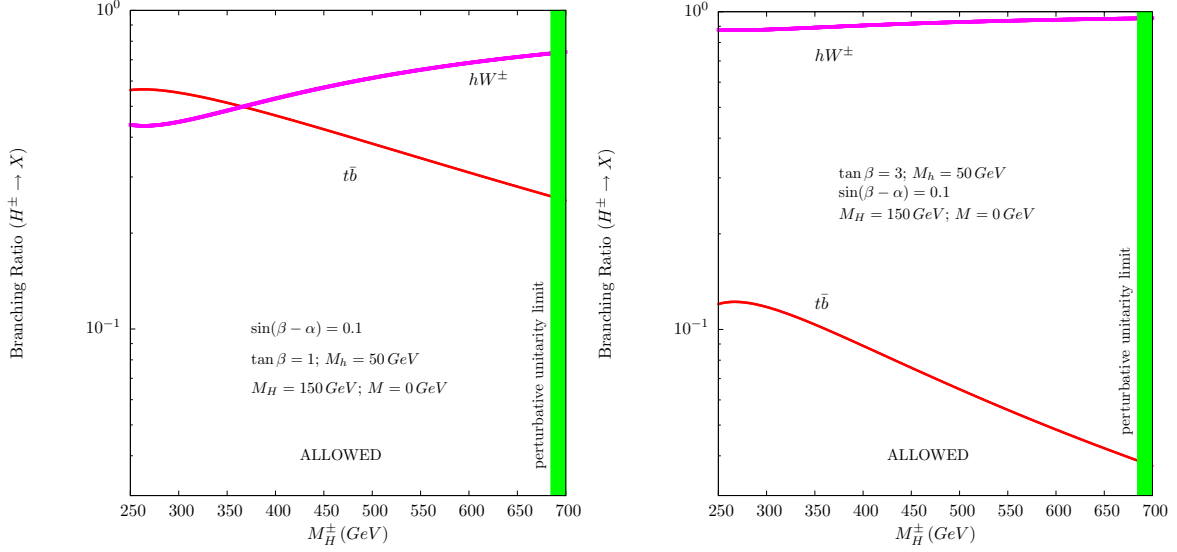


FIG. 6: H^\pm decays for $M_h = 50 \text{ GeV}$, $M_H = 150 \text{ GeV}$, $M_A = M_{H^\pm}$ and $\sin(\beta - \alpha) = 0.1$. On the left is the plot for $\tan\beta = 1$ while on the right we set $\tan\beta = 3$. Perturbative unitarity limits are shown.

The other extreme case, $\sin(\beta - \alpha) = 0.9$, is plotted in Fig. 7. In this case the H^\pm coupling to the heavier CP-even Higgs boson becomes dominant relative to the light Higgs case and the decay $H^+ \rightarrow W^+H$ is now the leading one for large values of $\tan\beta$. The ρ constraint could alternatively be enforced by $M_{H^\pm} \approx M_H$ because $\sin(\beta - \alpha) \approx 1$ as can be seen from the left plot in Fig. 1. In that scenario the HW^+ final state would be replaced by $H^+ \rightarrow AW^+$ which is independent of the value chosen for $\tan\beta$. Again, we take $M_H = 150 \text{ GeV}$, though this value has no bearing on the final result except when we

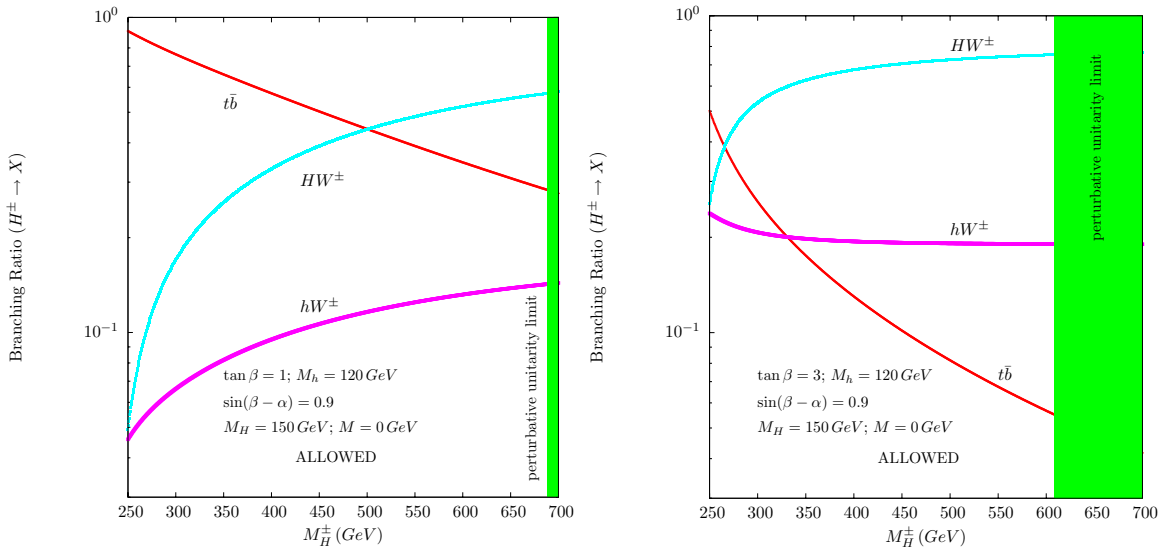


FIG. 7: H^\pm decays for $M_h = 120 \text{ GeV}$, $M_H = 150 \text{ GeV}$, $M_A = M_{H^\pm}$ and $\sin(\beta - \alpha) = 0.9$. On the left is the plot for $\tan\beta = 1$ while on the right we set $\tan\beta = 3$. Perturbative unitarity limits are shown.

are in a region of large $\tan\beta$ and large $\sin(\beta - \alpha)$. However, the large $\tan\beta$ region is excluded by the

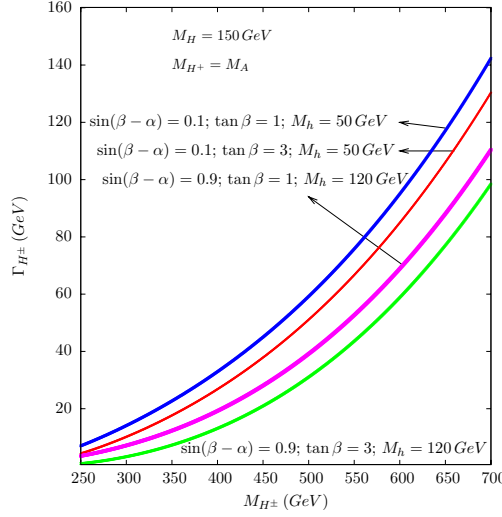


FIG. 8: Total width of the charged Higgs state H^\pm for the parameter values presented in Figs. 6 and 7.

perturbative unitarity constraints and therefore we will not consider this scenario. In Fig. 8 we show the total H^\pm width for the situations presented in Figs. 6 and 7. It is clear from the plot that the width does not depend so much on the parameters as happened for the previous cases. This is due to the fact that all channel types are already allowed starting from $M_{H^\pm} = 250 \text{ GeV}$.

For the mass regions considered in the plots, all MSSM scenarios predict an almost 100 % decay to tb . As stated in the introduction, the $H^\pm \rightarrow W^\pm h$ channel although kinematically possible in the MSSM, only occurs with sizable rates in a $\tan \beta$ region which is already excluded by experimental data. Therefore to distinguish a charged Higgs from 2HDM we should look for sizeable final states with one W boson and some other scalar.

V. CONCLUSIONS

We have highlighted that in a Type II 2HDM there exist Higgs-to-Higgs decays which are prevented from occurring in its SUSY version, the MSSM, owing to the fact that the latter imposes stringent relations amongst the masses of the H , A and H^\pm states, so that they are degenerate in mass over most of the parameter space. As these modes typically involve decaying Higgs states that are rather heavy, they could be primary means available at the LHC (and much less so at the Tevatron) to dispell the MSSM hypothesis that assumes that the sparticle states are very heavy and beyond the kinematical reach of the collider. An analysis of Higgs pair production in the same spirit is now also in progress [32].

APPENDIX A: YUKAWA COUPLINGS OF A TYPE II 2HDM

In this Appendix we present the Feynman rules for the Type II 2HDM Yukawa couplings. Hereafter, the label u refers to up-type quarks and neutrinos whilst d to down-type quarks and leptons. Also notice that the Goldstone bosons couple just like in the SM, so we do not report their fermionic interactions here. Finally, we define $\gamma_L = (1 - \gamma_5)/2$ and $\gamma_R = (1 + \gamma_5)/2$. Using notation already introduced (apart from V_{ij} being the Cabibbo-Kobayashi-Maskawa matrix element in the quark sector and equating to 1 in the lepton case), one has:

$$\begin{aligned}
\bar{u}_i u_i h: & -\frac{ig}{2M_W} \frac{\cos \alpha}{\sin \beta} m_{u_i} & \bar{d}_i d_i h: & \frac{ig}{2M_W} \frac{\sin \alpha}{\cos \beta} m_{d_i} \\
\bar{u}_i u_i H: & -\frac{ig}{2M_W} \frac{\sin \alpha}{\sin \beta} m_{u_i} & \bar{d}_i d_i H: & -\frac{ig}{2M_W} \frac{\cos \alpha}{\cos \beta} m_{d_i} \\
\bar{u}_i u_i A: & -\frac{g}{2M_W} \cot \beta m_{u_i} \gamma_5 & \bar{d}_i d_i A: & -\frac{g}{2M_W} \tan \beta m_{d_i} \gamma_5 \\
\bar{u}_i d_j H^+: & \frac{ig}{\sqrt{2}M_W} V_{ij} [\tan \beta m_{d_j} \gamma_R + \cot \beta m_{u_i} \gamma_L] & \bar{d}_i u_j H^-: & \frac{ig}{\sqrt{2}M_W} V_{ij}^* [\tan \beta m_{d_i} \gamma_L + \cot \beta m_{u_j} \gamma_R]
\end{aligned}$$

Acknowledgments The authors thank Koji Tsumura and Mayumi Aoki for useful discussions. Also, they acknowledge financial support from the PMI2 Connect Initiative in the form of a Research Cooperation Grant. SM thanks SK, YM and KY for hospitality in Toyama while the latter thank the former for the same reason in Southampton. RS is supported by the FP7 via a Marie Curie Intra European Fellowship, contract number PIEF-GA-2008-221707.

-
- [1] M. Drees, R. Godbole and P. Roy, “Theory and Phenomenology of Sparticles” (World Scientific Publishing Company, 2004).
 - [2] H. E. Haber and G. L. Kane, Phys. Rept. **117** (1985) 75.
 - [3] V. D. Barger, J. L. Hewett and R. J. N. Phillips, Phys. Rev. D **41** (1990) 3421.
 - [4] J. F. Gunion, H. E. Haber, G. L. Kane and S. Dawson, “The Higgs Hunter’s Guide” (Westview Press, 2000) [Erratum arXiv:hep-ph/9302272].
 - [5] A. Djouadi, Phys. Rept. **459** (2008) 1.
 - [6] S. Moretti and W. J. Stirling, Phys. Lett. B **347** (1995) 291 [Erratum-ibid. B **366** (1996) 451].
 - [7] A. Djouadi, J. Kalinowski and P. M. Zerwas, Z. Phys. C **70** (1996) 435.
 - [8] Z. Kunszt, S. Moretti, and W. J. Stirling, Z. Phys. C **74** (1997) 479.
 - [9] S. Moretti, J. Phys. G **28** (2002) 2567.
 - [10] S. Kanemura, Y. Okada, E. Senaha and C. P. Yuan, Phys. Rev. D **70** (2004) 115002.
 - [11] M. Aoki, S. Kanemura, K. Tsumura and K. Yagyu, in preparation; M. Aoki, S. Kanemura, O. Seto, arXiv:0807.0361 [hep-ph].
 - [12] S. Schael *et al.* [ALEPH, DELPHI, L3 and OPAL Collaborations], Eur. Phys. J. C **47** (2006) 547.
 - [13] V. M. Abazov *et al.* [D0 Collaboration], arXiv:0807.0859 [hep-ex]; CDF Collaboration, CDF Note 9322.
 - [14] A. Denner, R. J. Guth, W. Hollik and J. H. Kuhn, Z. Phys. C **51** (1991) 695.
 - [15] S. Eidelman *et al.* [Particle Data Group], Phys. Lett. B **592** (2004) 1.
 - [16] A. Pomarol and R. Vega, Nucl. Phys. B **413** (1994) 3.
 - [17] A. W. El Kaffas, O. M. Ogreid and P. Osland, arXiv:0709.4203 [hep-ph] and Phys. Rev. D **76** (2007) 095001.
 - [18] M. Krawczyk and J. Zochowski, Phys. Rev. D **55** (1997) 6968; A. Dedes and H. E. Haber, JHEP **0105** (2001) 006.
 - [19] See <http://lepewwg.web.cern.ch/LEPEWWG/>.
 - [20] See <http://www-sld.slac.stanford.edu/sldwww/sld.html>.
 - [21] D. S. Du, arXiv:0709.1315 [hep-ph].
 - [22] J. Rosiek, Phys. Lett. B **252** (1990) 135; W. Hollik and T. Sack, Phys. Lett. B **284** (1992) 427; M. Krawczyk and D. Temes, Eur. Phys. J. C **44** (2005) 435.
 - [23] P. H. Chankowski, M. Krawczyk and J. Zochowski, Eur. Phys. J. C **11** (1999) 661.
 - [24] K. Cheung and O. C. W. Kong, Phys. Rev. D **68** (2003) 053003.
 - [25] S. Kanemura, T. Kubota and E. Takasugi, Phys. Lett. B **313** (1993) 155.
 - [26] A. G. Akeroyd, A. Arhrib and E. M. Naimi, Phys. Lett. B **490** (2000) 119; J. Horejsi and M. Kladiva, Eur. Phys. J. C **46** (2006) 81.
 - [27] N. G. Deshpande and E. Ma, Phys. Rev. D **18** (1978) 2574; M. Sher, Phys. Rept. **179** (1989) 273; S. Kanemura, T. Kasai and Y. Okada, Phys. Lett. B **471** (1999) 182.
 - [28] I. P. Ivanov, Phys. Rev. D **75** (2007) 035001 [Erratum-ibid. D **76** (2007) 039902].
 - [29] P. M. Ferreira, R. Santos and A. Barroso, Phys. Lett. B **603** (2004) 219 [Erratum-ibid. B **629** (2005) 114].
 - [30] V. D. Barger, J. L. Hewett and R. J. N. Phillips, Phys. Rev. D **41** (1990) 3421.
 - [31] A. Djouadi, arXiv:0810.2439 [hep-ph].
 - [32] S. Kanemura, S. Moretti, Y. Mukai, R. Santos and K. Yagyu, in preparation.
 - [33] To the extent that, for masses of the heavy Higgs states above 200 GeV or so, a sort of decoupling occurs between these and the lightest Higgs boson of the MSSM, so that the latter resembles its SM counterpart.
 - [34] While the $H^\pm \rightarrow W^\pm h$ channel is kinematically possible in the MSSM, this only occurs with sizable rates in a $\tan \beta$ region which is already excluded by experimental data.
 - [35] For completeness, though not dealt with here, we identify as Type I the model where only the doublet ϕ_2

couples to all fermions; in a Type III [3] (also known as Type Y) model ϕ_2 couples to all quarks and ϕ_1 couples to all leptons; a Type IV [3] (also known as Type X [11]) model is instead built such that ϕ_2 couples to up-type quarks and to leptons and ϕ_1 couples to down-type quarks.